ISSN: 1231-4005
e-ISSN: 23540133
DOI: 10.5604/01.3001.0010.3091

A NOVEL DEVICE WITH VARIABLE FRICTION FOR SHOCK AND VIBRATION CONTROL

Tudor Sireteanu, Ana-Maria Mitu, Gheorghe Ghita, Adrian Niculescu

Institute of Solid Mechanics of Romanian Academy
Department of Dynamic Systems
Constantin Mille Street 15, 010141 Bucharest, Romania
tel.: +40213126736, fax: +40213126736
e-mail: anamariamitu@yahoo.com

Antoni Jankowski

Institute of Aviation
Krakowska Av. 110/114, 02-256 Warsaw, Poland
tel.: +48 228460011, fax: +48 228464432
e-mail: antoni.jankowski@ilot.edu.pl

Miroslaw Kowalski

Air Force Institute of Technology
Ks. Boleslawa Street 6, Poland
tel.: +48 261851303, fax: +48 261851313
e-mail: miroslaw.kowalski@itwl.pl

Abstract

In this article a passive system, which exploits the properties of the Coulomb friction and leads to high affordability of controlling shocks and vibrations by means of cheap devices is presented. The friction force developed by the proposed device is dependent on the motion stroke by convenient modulation of contact force between the elements of friction coupling. For providing the system self-centring properties or necessary vertical load capacity, coil springs can be incorporated into the device structure. The device hysteresis characteristic can be simply adjusted to comply with requirements of the considered application. A general mathematical model of device dynamic behaviour is developed and applied to shock and vibration isolation systems.

The article presents a novel passive device with variable friction which hysteresis force-displacement characteristics have "butterfly" shape, achieved by appropriate design of friction coupling. This shape of hysteresis loops can mitigate the drawbacks of constant friction devices. The schematic of mechanical systems to analyse the dynamic behaviour of shock and vibration isolation systems with variable friction device are shown.

Keywords: *variable friction, hysteresis, shock and vibration isolation, simulation*

1. Introduction

Friction dampers are considered as one of the most efficient energy dissipation. Compared with velocity-dependent devices such as viscous and viscoelastic dampers, friction dampers can provide sufficient initial stiffness as well as energy-dissipation capacity. The conventional friction devices develop constant friction force over the entire range of their stroke. The relative displacement across the device is largely restricted until the friction force is overcome. Therefore, the constant friction devices add initial stiffness to the structural system. The sudden variation of structural stiffness can lead to important shocks transmitted to the structure at the beginning of device relative motion. Additionally, the permanent high contact forces between the elements of friction coupling could amplificate these phenomena. Moreover, if a restoring force mechanism is not provided within the friction system, permanent deformation of the structure may exist after ceasing the applied excitation. To minimize the occurrence of such permanent displacements, some self-centring friction devices have been developed [1, 2]. The devices with variable friction were mainly used for semi-active control of vibration with different types of actuators to modulate the normal force applied on friction coupling [3-5]. In this article is proposed a novel passive device with variable friction which hysteresis force-displacement characteristics have “butterfly” shape [3], achieved by appropriate design of friction coupling. This shape of hysteresis loops can mitigate the drawbacks of constant friction devices. The dynamic behaviour of the proposed device is illustrated for SDOF isolation systems for shock and vibration.

2. Design principles and analytical model of variable friction device

The schematic of proposed device with variable friction is presented in Fig. 1 and 2 for two slightly different constructive solutions D1 and D2. The device D1 works mainly as damping system with a certain self-centring capacity, while the device D2 can be used as a compact system for isolation of shock and vibration with damping, self-centring and loading capacity.

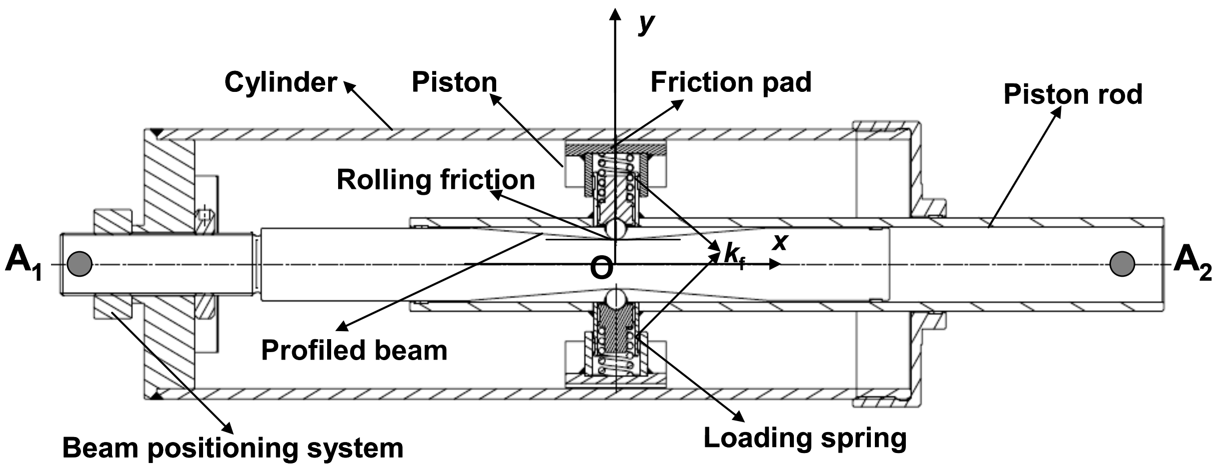

Fig. 1. The schematic of proposed damping system with variable friction D1

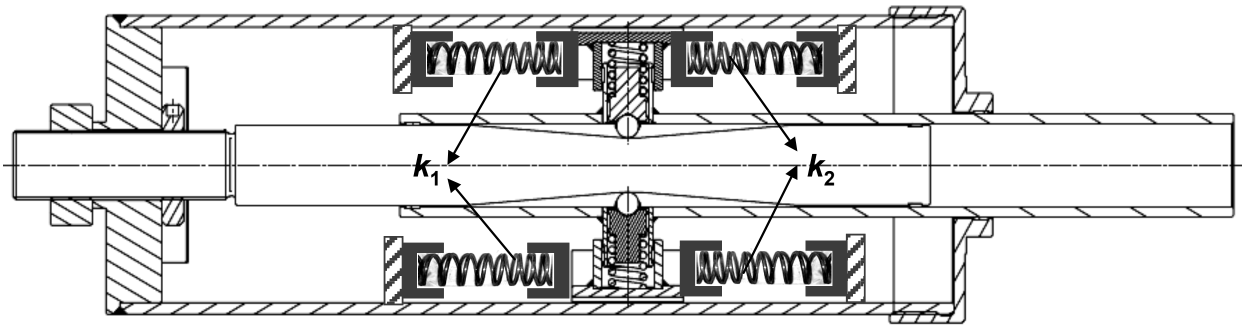

Fig. 2. The schematic of proposed system with variable friction for isolation of shock and vibrations D2

The stiffness coefficients k_f, k_1, k_2 represent the total stiffness of the spring pairs shown in this figures. If $k_1 = k_2 = 0$, the device D2 becomes the device D1.

The longitudinal profile of sliding beam surface with respect to its tangent in the intersection point with Oy is described by a function of the device relative displacement x between the mounting ends A1 and A2, having the following properties:

$$y = y(x); y(0) = 0; y(x) > 0,\ x \neq 0;\ y'(x)\operatorname{sgn} x > 0,\ y'(0) = 0 \cdot \tag{1}$$

Neglecting the rolling friction force, the hysteresis force developed by both devices during the sliding motion, can be expressed as the sum of a dissipative force and an elastic force

$$F_\mathrm{h}(x,\dot{x}) = F_\mathrm{d}(x,\dot{x}) + F_\mathrm{e}(x) \cdot \tag{2}$$

The dissipative force $F_\mathrm{d}(x,\dot{x})$ is the variable friction force given by:

$$F_\mathrm{d}(x,\dot{x}) = \mu F_\mathrm{n}(x)\operatorname{sgn}\dot{x} = \mu k_\mathrm{f}\left[y_0 + y(x)\right]\operatorname{sgn}\dot{x}, \tag{3}$$

where:

μ – friction coefficient,

$F_\mathrm{n}(x)$ – applied normal force on sliding friction coupling,

y_0 – compression of normal loading springs for $x = 0$.

The elastic force $F_\mathrm{e}(x)$ of D1 is projection of $F_\mathrm{n}(x)$ on the tangent of beam profile $y(x)$ providing a certain self-centring capacity:

$$F_\mathrm{e}(x) = k_\mathrm{f}\, y(x)\frac{y'(x)}{1 + y'^2(x)} \cdot \tag{4}$$

For D2, to this geometric elastic force must be added the elastic force developed by the incorporated springs. Since the pair of springs with total stiffness coefficients k_1 and k_2 are in series combination, the total device stiffness is:

$$k_{12} = \frac{k_1 k_2}{k_1 + k_2} \cdot \tag{5}$$

In what follows in case of device D2, the geometric elastic force (4) will be neglected. Therefore, the total force developed by the device D2 is given by:

$$F_\mathrm{h}(x,\dot{x}) = \mu k_\mathrm{f}\left[y_0 + y(x)\right]\operatorname{sgn}\dot{x} + k_{12}x. \tag{6}$$

Both D1 and D2 can be used in either vertical (as a suspension device) or horizontal position (as a bumper device), provided the sliding beam is placed in the medium position, $x = 0$, without dynamic loads. In case of D2, the stiffness coefficients k_1 and k_2 must provide the necessary self-centring and loading capacity of the suspension system. In the horizontal position, these springs can be mounted without any initial deflection. In this case, relation (6) becomes:

$$F_\mathrm{h}(x,\dot{x}) = \mu k_\mathrm{f}\left[y_0 + y(x)\right]\operatorname{sgn}\dot{x} + k_1 x(1 + \operatorname{sgn} x) + k_2 x(1 - \operatorname{sgn} x) \cdot \tag{7}$$

In vertical position, D1 must be mounted in parallel arrangement with an exterior spring.

The energy dissipated per cycle by both D1 and D2 devices, for an imposed harmonic motion $x(t) = X\sin\omega t$ between its mounting ends A1 and A2, is the area of the surface enclosed by hysteresis loop:

$$E_\mathrm{d} = \oint F_\mathrm{f}(x,\dot{x})\,\mathrm{d}x = \mu k_\mathrm{f}\omega X\int_0^{\frac{2\pi}{\omega}}\left[y_0 + y(X\sin\omega t)\right]\left|\cos\omega t\right|\mathrm{d}t. \tag{8}$$

In this article is considered the following form of the function $y(x)$ that describes the sliding beam profile:

$$y(x) = 0.5a_1 |x|^{\beta_1} (1 + \operatorname{sgn} x) + 0.5a_2 |x|^{\beta_2} (1 - \operatorname{sgn} x),$$
$$[a_i] = \mathrm{m}^{1-\beta_i}, \beta_i > 1, \ i = 1, \ 2. \tag{9}$$

Introducing (9) in (8), yields the analytical form of dissipated energy per cycle:

$$E_\mathrm{d} = 4\mu k_\mathrm{f} X \left[2y_0 + \frac{a_1 X^{\beta_1}}{\beta_1 + 1} + \frac{a_2 X^{\beta_2}}{\beta_2 + 1} \right]. \tag{10}$$

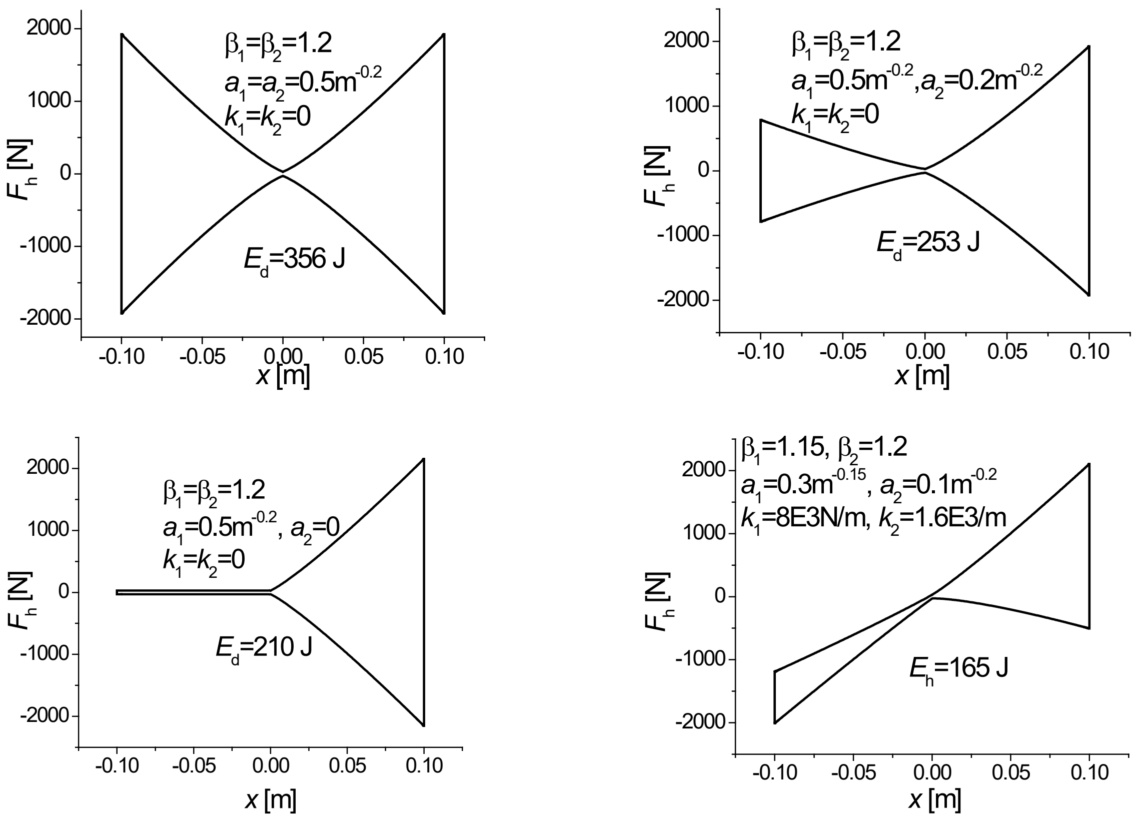

Fig. 3. Examples of hysteresis characteristics developed by the proposed device with variable friction

By modifying the parameters in (6), (7) and (9), one can obtain a large variety of rate independent hysteresis loops for imposed cyclic relative motions between the mounting ends of the device. In Fig. 3 are presented several examples of hysteresis loops, which can be developed by the proposed device for an imposed harmonic motion with $X = 0.1\,\mathrm{m}, \omega = 2\pi f, f = 1\mathrm{Hz}$, obtained by using (7) and (9). The values parameters $k_\mathrm{f} = 5 \cdot 10^4$ N/m, μ=0.3, $y_0 = 10^{-3}\,\mathrm{m}$ are the same for all displayed loops and only the parameters of the sliding beam profile and the stiffness coefficients k_1 and k_2 were modified such as the maximum developed force to be approximately 2000 N. The values of parameters and of corresponding dissipated energy per cycle are shown on each graph.

3. Application of device with variable friction D2 to shock and vibration isolation systems

The schematic of mechanical systems used to in this article to analyse the dynamic behaviour of shock and vibration isolation systems with variable friction device D2 are shown in Fig. 4 and 5, respectively.

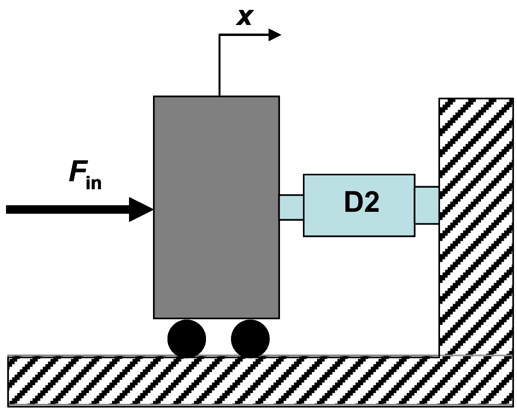

Fig. 4. Schematic of a shock isolation system with variable friction device D2

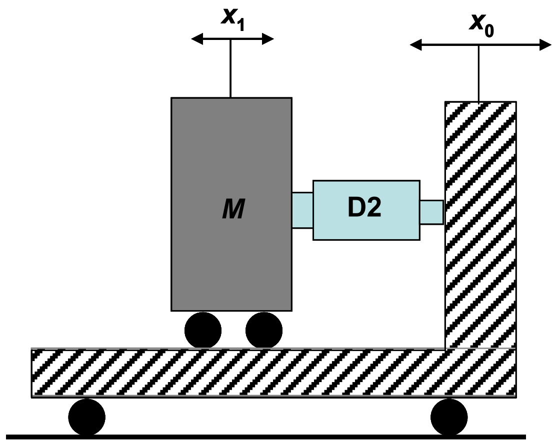

Fig. 5. Schematic of a vibration isolation system with variable friction device D2

3.1. Shock isolation system

The equation of motion of system shown in Fig. 4 is:

$$M\,\ddot{x} + F_{\mathrm{h}}\left(x,\dot{x}\right) = F_{\mathrm{in}}, \tag{11}$$

where:

F_{in} – the shock applied to mass M,

$F_{\mathrm{h}}\left(x,\dot{x}\right)$ – hysteresis characteristic of the device, obtained by introducing (9) in (7).

Using the notations:

$$\omega_{\mathrm{f}} = \sqrt{\frac{k_{\mathrm{f}}}{M}},\ \omega_i = \sqrt{\frac{k_i}{M}},\ i = 1,\ 2, \tag{12}$$

the equation of motion (11) can be written as:

$$\begin{gathered}\ddot{x} + f_{\mathrm{h}}\left(x,\dot{x}\right) = f_{\mathrm{in}}, f_{\mathrm{h}}\left(x,\dot{x}\right) = f_{\mathrm{f}}\left(x,\dot{x}\right) + f_{\mathrm{e}}\left(x\right),\ f_{\mathrm{in}} = \frac{F_{\mathrm{in}}}{M},\\ f_{\mathrm{f}}\left(x,\dot{x}\right) = \mu\omega_{\mathrm{f}}^2\left[y_0 + a_1\left|x\right|^{\beta_1}\left(1+\operatorname{sgn}x\right) + a_2\left|x\right|^{\beta_2}\left(1-\operatorname{sgn}x\right)\right]\operatorname{sgn}x,\\ f_{\mathrm{e}}\left(x\right) = 0.5\left[\omega_1^2 x\left(1+\operatorname{sgn}x\right) + \omega_2^2 x\left(1-\operatorname{sgn}x\right)\right].\end{gathered} \tag{13}$$

If a force of shock type $F_{\mathrm{in}}\left(t\right)$ is applied to mass M, the time history of the force transmitted to the system base is described by $M\cdot f_{\mathrm{h}}\left[x\left(t\right),\dot{x}\left(t\right)\right]$.

The dynamic behaviour of the shock isolation system, shown in Fig. 6, was obtained by numerical time integration of equation of motion (13), for the following input and values of device parameters:

$$f_{\mathrm{in}}\left(t\right) = \begin{cases} 0,\ 0 \le t < 1\mathrm{s}, \\ 1\mathrm{m/s^2},\ 1\mathrm{s} \le \mathrm{t} \le 1.1\mathrm{s}, \\ 0,\ 1{,}1s < t, \end{cases} \quad \begin{array}{lll} \mu = 0.2, & \omega_{\mathrm{f}} = 2\pi\cdot 0.25\mathrm{rad/s}, & y_0 = 0.001\mathrm{m}, \\ \beta_1 = 1.3, & a_1 = 0.5\mathrm{m}^{-0.3}, & \omega_1 = 2\pi\cdot 0.1\mathrm{rad/s}, \\ \beta_2 = 1.1, & a_2 = 0.3\mathrm{m}^{-0.1}, & \omega_2 = 2\pi\cdot 0.085\mathrm{rad/s}. \end{array}$$

The time histories shown in Fig. 6 illustrate the efficiency of using the proposed device with variable friction in shock isolation systems.

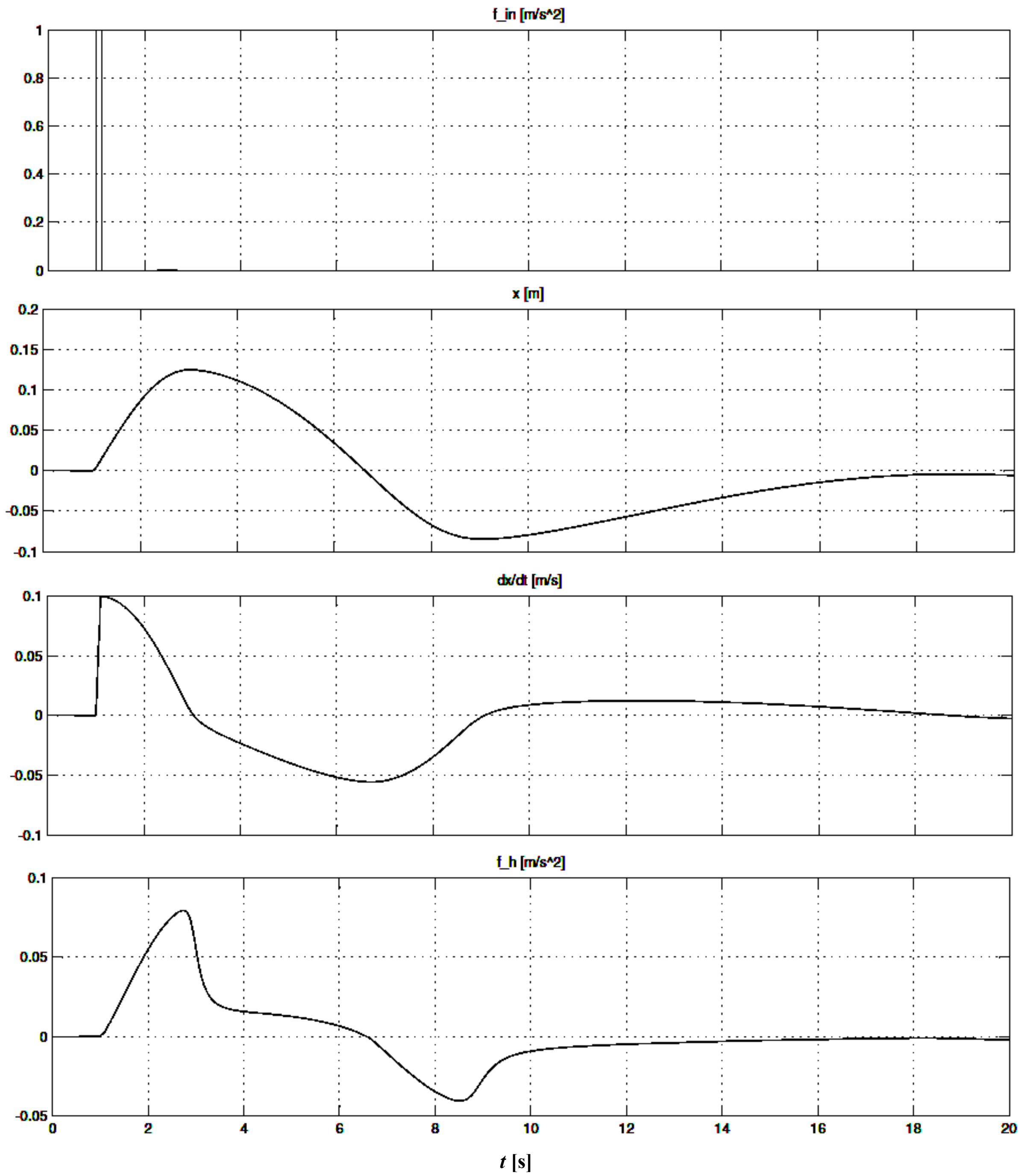

Fig. 6. The dynamic behaviour of device D2 used as a shock isolation system

3.2. Frequency response of vibration isolation system with variable friction

The motion of vibration isolation system shown in Fig. 5 is described by following differential equation:

$$M\,\ddot{x}_1 + F_{\mathrm{h}}\left(x, \dot{x}\right) = 0, \tag{14}$$

where:

$x_0\left(t\right)$ – imposed displacement of system base,

$x_1\left(t\right)$ – absolute displacement of sprung mass with respect to static equilibrium position,

$x\left(t\right) = x_1\left(t\right) - x_0\left(t\right)$ – relative displacement.

Using the notations given in (12) and (13), equation (14) can be written as:

$$\ddot{x} + f_{\mathrm{h}}\left(x, \dot{x}\right) = -\ddot{x}_0. \tag{15}$$

For a symmetric hysteresis characteristic of the vibration isolation system, $f_{\mathrm{h}}\left(x, \dot{x}\right)$ is obtained from (13) by letting $a_1 = a_2 = a$, $\beta_1 = \beta_2 = \beta$, $\omega_1 = \omega_2 = \omega_{\mathrm{n}}$.

The acceleration transmissibility factor of the considered vibration isolation system was obtained by sweeping the frequency of the harmonic input $\ddot{x}_0\left(t\right) = X_0 \sin \omega t$ in one fifteenth-octave sequence $\omega_k = 2^{(k-1)/15}\omega_1$, $\omega_1 = 0.1\pi$, $k = \overline{2,132}$, for constant value of amplitude X_0. The values $A_{\ddot{x}_1}\left(\omega_k\right)$ of transmissibility factor for r.m.s. acceleration are given by:

$$A_{\ddot{x}_1}\left(\omega_k\right) = \frac{\sigma_{\ddot{x}_1}\left(\omega_k\right)}{\sigma_{\ddot{x}_0}} = \frac{\sqrt{2}\,\sigma_{\ddot{x}_1}\left(\omega_k\right)}{X_0}, \tag{16}$$

where $\sigma_{\ddot{x}_1}\left(\omega_k\right)$ are the r.m.s. of the absolute acceleration $\ddot{x}_1\left(t\right)$ obtained by numerical simulation.

The transmissibility factor of r.m.s. acceleration of vibration isolation system with variable friction was compared with those obtained for a SDOF linear system with natural frequency ω_{n} and different values of relative damping coefficient ζ. The following values of parameters used in numerical simulations:

$$\mu = 0.2,\ \omega_{\mathrm{k}} = \omega_{\mathrm{n}} = 2\pi\,\mathrm{rad/s},\ \beta = 1.1,\ a = 5\mathrm{m}^{-0.1},\ y_0 = 0,\ X_0 = 1\mathrm{m/s}^2 \text{ and } X_0 = 2\mathrm{m/s}^2.$$

The results are presented in Fig. 7.

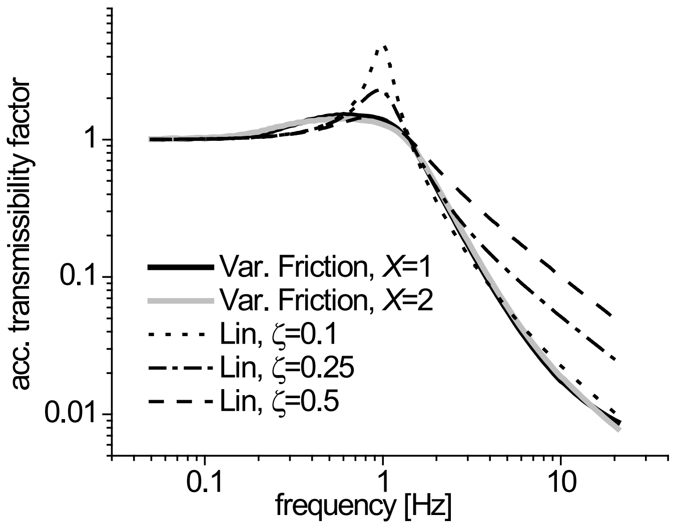

Fig. 7. Transmissibility factors of vibrations isolation systems with variable friction and of linear system

The plots shown in Fig. 7 show that the vibration isolation system with variable friction behaves like a linear system with almost critical relative damping in the resonance frequency range and like a linear system with low relative damping for higher input frequencies. Since the value of parameter β is slightly different from 1, the equation (15) is almost piece-wise linear. In case of piece-wise linear system the r.m.s. output transmissibility is independent of the input amplitude X_0 [4]. This property, highlighted by the results presented in Fig. 7, is very convenient for calculation of system r.m.s. output for inputs with more complex frequency spectra than the harmonic ones.

Acknowledgment

The work behind this article has been financially supported by The Executive Agency for Higher Education, Research, Development and Innovation Funding (UEFISCDI) through the research contract 112/2014. The support is gratefully acknowledged.

References

[1] Christopoulos, C., Tremblay, R., Kim, H.-J., Lacerte, M., *Self-Centering Energy Dissipative Bracing System for the Seismic Resistance of Structures: Development and Validation,* Journal of Structural Engineering, Vol. 134, No. 1, pp. 96-107, 2008.

[2] Ozbulut, O., Hurlebau, S., *Re-centring variable friction device for vibration control of structures subjected to near-field earthquakes*, Mechanical Systems and Signal Processing, Vol. 25, pp. 2849-2862, 2011.

[3] Fujita, T., *Semi-active control of base isolated structures*, The Active Control of Vibration, IUTAM Symposium Bath, pp. 289-295, UK 1994.

[4] Stammers, C. W., Sireteanu, T., *Vibration control of machines by use of semi-active dry friction*, Journal of Sound and Vibration, 209(4), pp. 671-684, 1998.

[5] Guglielmino, E., Sireteanu, T., Stammers, C.W., Ghita, Gh., Giuclea, M., *Semi-active suspension control, Improved vehicle ride and road friendliness*, Springer-Verlag London 2008.

[6] Sireteanu, T., Mitu, A.M., Ghita, G., *Passive and semi-active bracing systems for seismic protection: a comparative study*, Romanian Journal of Acoustics and Vibration, Vol. XII, Iss. 1, pp. 49-56, 2015.